Symmetry: Culture and Science
Vol. 19, No. 4, 233-247, 2008

SYMMETRY OF NANOSTRUCTURES IN PHYSICS

GRAVITATION SYMMETRY TEST

Alan M. Schwartz

. *E-mail*: xenophage@gmail.com

Abstract: *Gravitation theories allow isotropic or chiral vacuum backgrounds in the massed sector. Atomic mass distribution quantitative parity divergence can be calculated to large volumes in periodic crystals. It is shown that a parity Eötvös experiment opposing single crystal solid spheres of enantiomorphic space groups* $P3_121$ *and* $P3_221$ *quartz may empirically falsify isotropic vacuum and the Equivalence Principle without contradicting prior (achiral) observations in any venue at any scale, and should be performed.*

Keywords: PACS: 04.80.Cc, 11.30.Er (Experimental tests of gravitational theories; charge conjugation, parity, time reversal, and other discrete symmetries)

Received: 09 April 2009 ; *Accepted*: 30 May 2009

I. INTRODUCTION

Contemporary physical theory arises from the "unreasonable effectiveness of mathematics" (Wigner, 1960). Fundamental symmetries evolve then cool to elicit contents' phase transitions and observables whose mirror images should be identical. In truth, weak exchanges display chiral asymmetries. Lee and Yang (1956) demonstrated Weak interaction parity violation. Gravitation is 10^{-25} Weak interaction strength. It is modeled not to allow or to allow parity violation (Contaldi et al., 2008). Two novel empirical tests are proposed.

The weak field limit of pseudo-Riemannian spacetime is homogeneous and isotropic (an inertial frame), hence metric gravitation embedded. Einstein's elevator (Einstein, 1907) demands the (weak) Equivalence Principle (EP): All local centers of mass vacuum free fall along identical (parallel displaced) minimum action trajectories independent of composition and internal structure. Gravitational (m_g) and inertial (m_i) masses are indistinguishable. General relativity (GR) appears to be exact. No EP violations are reported.

Ashtekar and thereafter (Mercuri, 2006) recrafted formally achiral GR from a chiral Lagrangian (a tetrad and a complex self-dual connection as independent variables). Lorentz group Lie algebra separated into dextral (anti-self-dual) and sinistral (self-dual) copies of *SO*(3). Neutrino and allied chiral consequences emerged. No massed sector chiral vacuum background tests were proposed.

Weitzenböck spacetime contains EP = true. Separation of gravitation from inertia elicits teleparallel gravitation (Aldrovandi et al., 2008a). This additionally describes EP = false with gravitation connected through torsion (Aldrovandi et al., 2008b), allowing a massed sector chiral vacuum background. It would be inert in the massless sector (photons do not configure); to achiral, to unresolved (racemic), or to resolved low amplitude parity divergent mass distributions. Fitting a tight right shoe compared with its left shoe is compelling. Each compared with a sock together identify the sense of vacuum chirality. Calorimetry data tolerate EP chiral mass divergence of $2|m_g - m_i|/|m_g + m_i| < 10^{-12}$ (benzil ΔH_{fusion}, Section V). Eötvös experiments have 5×10^{-14} sensitivity (Schlamminger et al., 2008).

The Nordtvedt effect is not observed (Schlamminger et al., 2008). *L*-amino acids (protein) and *D*-sugars (cellulose) cancel a parity Nordtvedt effect. Polarized electron spin and orbital angular momentum test masses validate the EP (Will, 2005). GR exactly describes 1.74 solar-mass pulsar PSR J1903+0327 in a 95.17-day 0.437-eccentricity orbit with its 1.05 solar-mass star companion. 27% vs. 1.4×10^{-4}% gravitational binding energy, 1.8×10^{11} vs. ~30 surface gees, 2×10^{8} gauss vs. ~5 gauss magnetic field, superconductive compressed neutrons and exotica vs. proton-electron plasma; pulsar equatorial spin >11% lightspeed validate the EP within observational error (Heckel et al. 2006; Hou et al., 2003; Ritter et al., 1990). Spacetime geometry challenged by chiral atomic mass distributions remains undetermined.

II. SYMMETRIES AND PROPERTIES

Not all symmetry-property couplings via Noether's theorem are strong EP tests. Internal symmetries' corresponding properties can transform fields amongst themselves leaving translation and rotation unchanged. Local gauge transformation in 4D spacetimes may not cancel all local degrees of freedom to make the local gauge-field vanish. However, necessarily small EP violations will be further deeply diminished: Contrasts of baryon number, charge conjugation, electric charge, lepton number, hypercharge, weak hypercharge, electroweak force, isospin, weak isospin, *G*-parity, *R*-parity, quark color, quark flavor.

External symmetries' properties connect to translation and rotation. Parity is the only external symmetry with no continuous approximation (time reversal is inaccessible re boosts; charge conjugation is an internal symmetry). It is excluded from Taylor expansions, smooth Lie groups, and Noether's theorem. Invariance of a linear differential operator under a discrete symmetry requires a partial differential equation, here invariant under reflection, to possess solutions that are also invariant. If **G** is the Hermitian generator of nontrivial unitary operator **U** (e.g., parity), then if **U** commutes with Hamiltonian **H**, then so does **G**: [**H**,**G**] = 0. If **U** commutes with **H** it is a symmetry (invariants being tensor contractions of the basis of the vector space of **G**, the equivalent of scalars but in the space of symmetry operators).

Parity as symmetry couples to property outside Noether's theorem. It offers EP violation outside theory and observation restricting continuous symmetries' consequences. Invariants on the algebra of symmetries generated by discrete symmetries are difficult to determine, requiring Hilbert's theory of algebraic invariants and invariant orbits in an algebra or a group. Explicit association between such invariants and discrete symmetries is unclear. Experiment will be definitive.

True chiral systems exist in two distinct enantiomorphic states interconverted by space inversion but not by time reversal combined with any proper spatial rotation (Barron, 1981). Chirality is an emergent phenomenon requiring at least four non-coplanar points in 3-space. The ratio of emergent scale to experimental scale is consequential. Quantitative geometric parity divergence of an atomic mass distribution evolves with increasing radius despite macroscopic crystal lattice volume being self-similar to its angstrom-dimensioned unit cell.

EP parity divergence is geometric (Petitjean, 2003) not compositional or electronic. Optical chirality (time-reversal even, imaginary part of the complex gyrotropy tensor) is progressive rotation of the plane of linearly polarized light with passage through a medium. It is an artifact of orbitals and interrogation frequency (Jerphagnon and Chemla, 1976; Glazer and Stadnicka, 1986). 2-Norbornanone has $[\alpha]_D = 29.8°cm^3$/g-dm (Crawford et al., 2007; Wiberg et al., 2006). 2-Norbornenone has $[\alpha]_D$ = 1146.°cm^3/g-dm. The molecules are essentially superposable except for olefinic hydrogens. Silver thiogallate, $AgGaS_2$ with non-polar achiral tetragonal space group I-42d, has 522°/millimeter optical rotation along [100] at 497.4 nm (Etxebarria, 2000). α-Quartz has no measurable optical chirality 56.16° from crystallographic [0001] (Szivessey and Münster, 1934).

Local measures of parity divergence may not sufficiently describe atomic mass distribution in a macroscopic object. Identical homochiral units combine to achirality in *La Coupe du Roi* (Hargittai and Hargittai, 1995). Explicit calculation of large volumes is required. Test masses must tolerate minor impurity and structural imperfection without major parity divergence degradation.

Resolved enantiomers in prior enthalpy of racemization, solution, or combustion studies did not meet parity divergence geometric criteria (Pagni and Compton, 2002). Biological homochirality sourced by $8x10^{-12}$ eV parity-violating energy difference Z^0-exchange in atoms (versus kT = 0.0257 eV at 298 K) is unpalatable (Keszthelyi, 2003, Quack, 2002). Big Bang selection of matter over antimatter requires violated conservation of baryon number and lepton generation number, plus C- and CP-symmetry violations. Biological homochirality requires a consistent global mechanism. A massed sector chiral vacuum test should be performed.

III. QUANTITATIVE GEOMETRIC PARITY DIVERGENCE

Invert a thin, pliable, unstretchable left glove into a right glove. Aside from closed topologies (e.g., a glove balloon), a d-dimensional set with $N \geq (d + 2)$ points can continuously transform into its mirror image absent achiral intermediates (Mezey, 1995). Mass distribution quantitative chirality requires a continuous function including extreme opposite values and zero without forced passage through zero during inversion.

The International Union of Crystallography defines a crystal as “any solid having an essentially discrete diffraction diagram” including periodic, quasiperiodic, and

modulated lattices; incommensurate, misfit, or composite structures, and polytypes. All relative atom coordinates within a periodic crystal are known given unit cell space group, axis lengths and angles, and unique fractional coordinates of contents.

Avnir's semi-empirical analysis of α-quartz (Yogev-Einot and Avnir, 2003) does not easily adapt to calculating macroscopic volumes of crystal lattice. Petitjean's *ab initio* public domain software QCM (Petitjean, 1999) generates χ (normalized parity divergence, values in [0;1]), COR (number of graph automorphisms), and DSI (self-similarity index). Given input atom coordinates, QCM outputs are rapidly calculated from four through ~1500 atoms, typically at angstrom radius increments. All four combinations of $\chi \geq 0$ and DSI ≥ 0 can exist. COR cannot exceed the number of graph automorphisms, maximally n! for a graph of n nodes wherein every node connects to (n – 1) nodes. Rapidly consistent $\chi \rightarrow 1$, COR =1 (identity element only) and DSI = 0 (zero self-similarity) with increasing radius to eventually include 1100 or more identifies a candidate crystal structure. COR > 1 or DSI > 0 beyond a few contained unit cells is disqualifying.

Chirality can emerge from atom composition (e.g., isotopic or isomorphous substitution in a crystal lattice) or pure geometry (relative location in space). No observable violates the EP. All atoms are gravitationally anonymous unit masses, chemical bonding is invisible. Atoms were assigned unit mass and were input without regard to chemical bonding. QCM input file format does not change output but it can affect run time. *.xyz format run time scales as n!. Minimum run times emerge from HyperChem *.hin format with atoms linearly spiraling out from the center to the periphery of the structure. Three random crosslinks are added to assure calculation exit.

A countable set of points with finite moments of inertia overall has three principal moments of inertia locating its center of mass. The set's parity inversion (e.g., all coordinates reversed in sign) is created. One set is translated and rotated (quaternions) to minimize $D^2/4T$ in Eq. (1), giving coincident centers of mass with overall minimum distance between corresponding points. If the sets superpose, the original set was achiral and $\chi = 0$. Otherwise, χ is globally minimum for all rotations (R) and translations (t) for all pairwise correspondences or graph automorphisms (P),

$$\chi = (d)[\mathrm{Min}_{\{P,R,t\}} D^2]/4T \qquad (1)$$

where d is the Euclidean dimension, D^2 is the sum of the N squared-distances between the set and its parity inversion for a fixed pairwise correspondence with coincident

centers of mass, and T is the geometric inertia of the set. A set of points and its parity inversion have the same χ value.

Resolved chiral alkanes (no interactive chromophores, no serially repeated rotators) typically exhibit $[\alpha]_D$ of a few degrees cm^3/g-dm. Twistane, $C_{10}H_{16}$ with $\chi = 0.708928$, has $[\alpha]_D = 446°cm^3$/g-dm or a molar specific rotation of 60,800°. Designed skeletal $\chi = 1$ [6.6]chiralane, $C_{27}H_{28}$ with $\chi = 0.982423$, has calculated $[\alpha]_D = 692°\ cm^3$/g-dm or a molar specific rotation of 244,000° (Nakazaki et al., 1982; Autschbach, …; Schwartz and Petitjean, 2008). Resolved 2-norbornenone (above) with exceptional chromophore interaction has a molar specific rotation of 124,000°.

A subset of QCM without COR and DSI graph automorphisms enumeration was adapted as BigCHI. Given QCM-qualified crystal structure data, radius calculation ranges, and radial sampling increments BigCHI will grow arbitrarily large crystal lattice volumes and process some 10^7 atoms/CPU-second for χ in a desktop computer. Parallelized CHIpir runs in cluster and cloud computing (Hooper et al., …). χ at usefully small radius increments is unremarkably calculated in long_double_precision for crystal lattice volumes containing more than $4x10^{17}$ atoms.

With only the identity automorphism allowed (COR = 1, DSI = 0), χ is a function of the eigenvalues of the inertia matrix. It was suggested (Smith, …) that χ is then a connection among eigenvalues, special functions, their representation theory with solid angles, and exponentials of fractions of pi at a characteristic scale. Eq. (2) emerges from Petitjean's analysis, then modeled as Eq. (3) that is testable,

$$\log(1-\chi) = (-2/3)[\log(\text{atoms})] + \text{intercept} \qquad (2)$$

$$\log(1-\chi) = -2[\log(\text{radius, Å})] + [\pi(180-\Phi)/60] - \pi \qquad (3)$$

The intercept is the smallest solid angle subtended by the vertex angle Φ of a polyhedron (the supplement of its dihedral angle) within a crystallographic screw axis, defined by three consecutive atoms in the formula unit. The smallest radial increment "r" at radius "R" (both in angstroms) that includes new atoms and thereby potentially alters χ empirically varies as $r \approx 10/R^2$. Small radius sampling density is limited by χ change with radius increment. Large radius sampling density is limited by calculation time increasing as $(\text{radius})^2$. Graphic intercept rapidly stabilizes at high sampling densities to within ~10% of modeled value. When every radius increasing included

atoms is sampled, the equation is exact. Only the first of identical χ values is retained when a radial increment does not include more atoms .

A crystallographic space group is a group of automorphisms with a bounded set of points. Chiral crystal structures (65 Sohncke space groups of 230 3-space periodic space groups) are insufficient for constructing opposite parity test masses (Flack, 2003). Eleven pairs of enantiomorphic space groups in the 65 include three pairs containing both senses of screw axes and five pairs containing racemic (2_1, 4_2, or 6_3) screw axes: $P3_112$ / $P3_212$, $P3_1$ / $P3_2$, and $P3_121$ / $P3_221$ are robust. The first are lamellar solids (e.g., $CrCl_3$) difficult to grow as large single crystals or machine. $P3_1$ / $P3_2$ with neaar zero vapor pressure are rare (e.g., glycine γ-poymorph). $P3_121$ / $P3_221$ are the α-quartz group – quartz, berlinite and $M(+3)A(+5)O_4$ analogues (M = B, Al, Fe, Ga; A = P, As), cinnabar, tellurium, selenium, benzil, and others. All $P3_121$ / $P3_221$ analyzed to date meet QCM $\chi \rightarrow 1$, COR =1, DSI = 0 criteria.

Light atoms (H, Be, Li) have large thermal anisotropies in their determined crystal structures. Hydrogen atoms are inserted unless neutron diffraction (e.g., deuterated analogues) explicitly locates them. Commercial cultured quartz is the prime candidate to test for massed sector vacuum chirality.

IV. REDUCTION TO PRACTICE

EP parity tests require contrasted identical composition and macroscopic form test masses such that

1) Essentially 100% of test mass rest mass is active mass.

2) Parity divergence calculation is *ab initio* from relative atom coordinates only.

3) Maximum parity divergence occurs: $(1 - \chi) < 10^{-10}$, COR=1, DSI=0. Respective inertia matrices are proportional to the diagonal identity matrix, (1,0,0)(0,1,0),(0,0,1), its three pairs of off-diagonal terms (products of inertia) being zero, $I_x = I_y = I_z$. QCM theory extends to a continuum of points (Petitjean, 2002).

4) A test mass has a sub-nanometer chirality emergent scale gaplessly accumulating in-phase to centimeter dimensions and gram masses (self-similar periodic single crystal).

5) Quality single crystals can be grown and machined.

6) χ resists decrease given sparse noise: impurities, vacancies, interstitials, dislocations, mosaicity.

7) Both resolved parities are available absent a ferroelectric phase; allotropy, polymorphism, polytypism, magnetic inclusions, amorphous volumes, disinclinations; electrical (Dauphiné) twinning, and optical (Brazil) twinning.

8) Parity experiments run in unmodified composition apparatus with unchanged protocols pre-qualified for control experiment zero net output within experimental error.

X-ray (scattered by electrons) and neutron (scattered by nuclei) α-quartz diffraction structures are identical within experimental error. Mass has consistent coordinates, listed in Table I.

Diffraction method	Unit cell axes, Å *a,b*	*c*	Unit cell volume, nm^3	Fractional coordinates *x/a*	*y/b*	*z/c*		Vertex angle
X-ray (Kihara, 1990)	4.9137	5.4047	0.11301	0.4697	0.0000	1/6	**Si**	110.56°
				0.4133	0.2672	0.2855	**O**	
neutron (Wright and Lehmann, 1981)	4.9134	5.4052	0.11301	0.4701	0.0000	1/6	**Si**	110.53°
				0.4136	0.2676	0.2858	**O**	

Table I: Coordinates of $P3_221$ α-quartz atoms and nuclei at 298°K.

Inhomogeneity (atom or not atom), unit cell anisotropy (unique c-axis), and dependence of χ upon inertial moments give substantial fluctuations around a uniform trend as sample radius increases. χ values for increasing radius single crystal spherical balls of α-quartz or benzil (More et al., 1987) give slopes and intercepts consistent with Eq. (3). Pearson correlation is -0.9945 for α-quartz and -0.9880 for benzil.

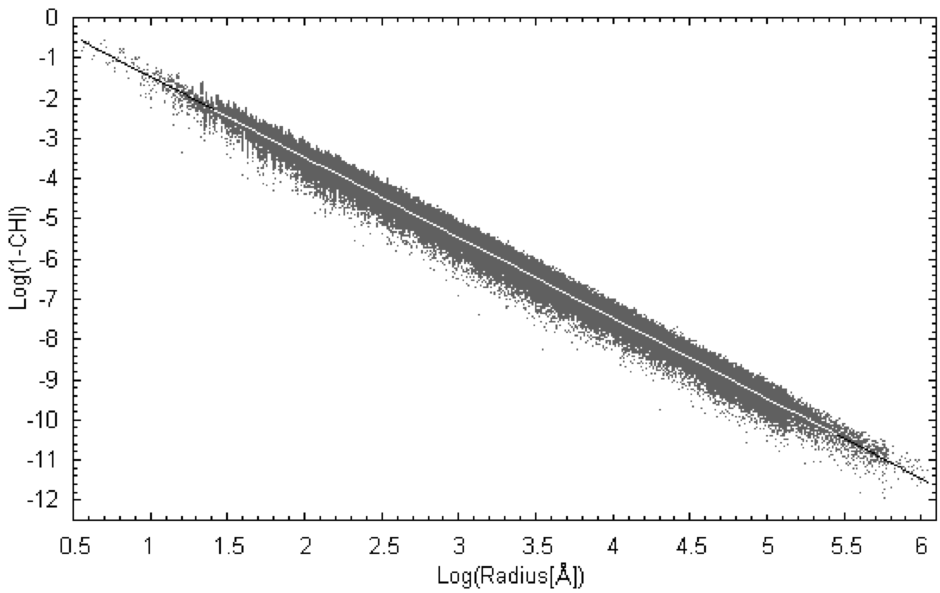

Figure 1: α-Quartz approach to $\chi = 1$ by radius to 4.44×10^{17} atoms; 90,386 points.

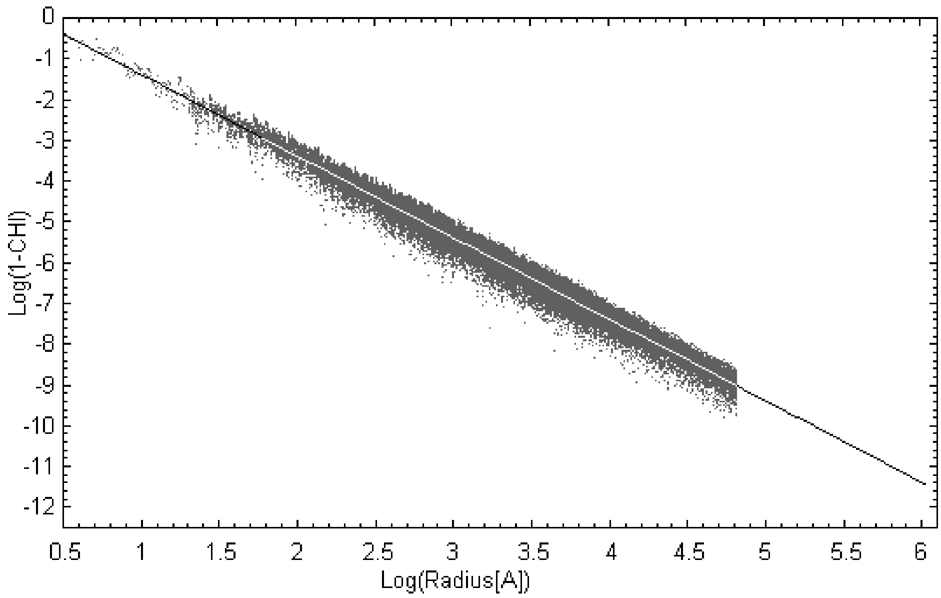

Figure 2: Benzil approach to $\chi = 1$ by radius to 1.07×10^{14} atoms; 53,213 points.

Fitted slopes and intercepts rapidly stabilize at high sampling densities, Table II. Parity divergence arising from macroscopic form fails at smaller than pitch length. α-Quartz SiO_3 chirality emergent scale is within a 0.304 nm diameter sphere. Benzil (C=O)-(C=O) torsion angle is within a 0.313 nm diameter sphere.

Crystal lattice	Lattice volume/atom, nm^3	Vertex angle, Φ	Modeled intercept, slope	Graphic intercept, slope	$(1 - \chi)x10^{15}$, diameters 1.5 cm Eötvös	3 mm calorimetry
α-quartz	0.01256	O-Si-O	0.49428,	0.5342,5	0.5548	model
SiO_2		110.56º	-2 exactly	-2.00000	0.6083	graph
benzil	0.01070	(C=O)-(C=O)	0.58643,	0.6113,1	model	17.15
$(C_6H_5CO)_2$		torsion angle 108.80º	-2 exactly	-2.00067	graph	17.96

Table II: Modeled and graphic fits of log(1 - χ) versus log(radius).

V. PARITY EÖTVÖS AND PARITY CALORIMETRY EP TESTS

Geocenter orbital acceleration varies from 0.6133 cm/sec^2 03 January 2010 perihelion (day/month/year: 03/01/11, 05/01/12, 02/01/13) to 0.5737 cm/sec^2 06 July 2010 aphelion (04/07/11, 05/07/12, 05/07/13) averaging 0.5930 cm/sec^2 at one astronomical unit (…, 2001). Given World Geodetic System 1984, 44.95º latitude affords maximum 1.693 cm/sec^2 horizontal component of Earth's inertial spin at sea level. Sea level gravity is 980.6 cm/sec^2 (inactive in the experiments). Small imposed accelerations demand large contrasted property concentration and divergence for detectable EP violation of any type or origin.

Active test mass composition properties are small fractions of total mass. Their paired difference is no more than 0.2 mass-% net divergence. Essentially 100% of extremal parity test mass is actively divergent: nuclear mass (arguably plus position-averaged non-valence electrons' mass), presented in Table III.

An Eötvös torsion pendulum is the EP test gold standard. A symmetric ~6 cm diameter rotor is vertically suspended from a meter of typically 20 µm diameter tungsten filament in an isolated ultra-high vacuum chamber. It carries two weight- and moments of inertia -balanced sets of 180°-opposed test masses totaling ~40 grams. EP violation exerts diurnal nanoscopic periodic torque with interferometric rotation detection as the Earth orbits and rotates. Composition tests null to $5x10^{-14}$ difference/average.

Property	Fraction of rest mass
enantiomorphic crystal	99.9726% quartz
geometric parity divergence[a]	99.9713% benzil
Nuclear binding energy (low Z)	0.76% ^{4}He
Neutron versus proton mass	0.14%
Electrostatic nuclear repulsion	0.06%
Electron mass	0.03%
Unpaired spin mass	0.005% ^{55}Mn[b]
Nuclear antiparticle exchange	0.00001%
Weak Force interactions	0.0000001%
Gravitational binding energy	0.000000046% Earth[c]
(Nordtvedt effect)	0.0000000019% moon

[a] (nuclear mass)/(atomic mass) weighted for isotopic abundance

[b] Modeled as the aligned undecatiplet

[c] Iron core rather than homogeneous body

Table III: Single body (active mass)/(rest mass).

A parity Eötvös experiment (Schwartz, 2004) contrasts enantiomorphic space groups $P3_121$versus $P3_221$ quartz (average atom weight = 20.028) solid single crystal spheres (no direction bias). Hemiparity Eötvös experiments contrast α-quartz and amorphous fused silica test masses. Fused silica's smaller density, 2.649 and 2.203 g/cm^3 respectively, requires 0.878% undersized radius with total mass deficit restored by 19.3 g/cm^3 gold plating to full radius. In the same space groups cinnabar (Auvray and Genet, 1973) (average atom weight = 116.33, difficult to grow) or compositionally homogeneous tellurium (Adenis et al., 1989) (average atom weight = 127.60, tellurium breath) offer heavy atom alternatives. A chiral anisotropic vacuum background is detected with the same protocol as a composition Eötvös experiment.

Benzil, C_6H_5-(C=O)-(C=O)-C_6H_5, is an achiral flat molecule molten, gas phase, or in solution. Solid state lattice forces twist the molecules and align them into homochiral helices along a crystal's c-axis. Helices parallel stack into a triangular lattice, space groups $P3_121$ or $P3_221$. Crystal melts are achiral and indistinguishable. If opposite parity crystal inertial and gravitational masses diverge through diastereotopic interaction with a chiral vacuum background, that divergence must end when mass distribution parity divergence vanishes through melting. Mass divergence will disappear as heat, $\Delta m_g c^2$ or $\Delta m_i c^2$, incrementing the nominal $\Delta H_{\mathrm{fusion}}$ of powdered racemic benzil.

Hard by 45° latitude, two horizontally abutted differential scanning calorimeters' sample ports define a north-south line. Each holds a ~3 mm diameter ~17 mg benzil

single crystal sphere with sample carriers crimped against sublimation. One sample port consistently contains one crystal in space group $P3_121$ and the other sample port one crystal in $P3_221$. ΔH_{fusion} are simultaneously run. New crystals run at half-hour intervals from 0500 hrs to 2000 hrs inclusive local time. If $\Delta\Delta H_{\text{fusion}} \neq 0$ within experimental error, repeat the run the next day with east-west alignment. $\Delta\Delta H_{\text{fusion}}$ will have a six hour phase shift on the second day. Controls are ΔH_{fusion} of finely powdered racemic benzil.

There are four possible outcomes for a parity calorimetry experiment in benzil:

1) No net signal. $\Delta\Delta H_{\text{fusion}} = 0$. Enantiomorphic single crystal ΔH_{fusion} are identical to that of powdered racemic benzil. Values do not change versus time of day and *N-S* or *E-W* geographic orientation.

2) $P3_121$ and $P3_221$ crystals consistently fit with different energies into chiral vacuum. The melts are achiral and identical. Opposite parities of chemically identical crystal melting to the common state must display different enthalpies of fusion. At least one ΔH_{fusion} will be different from that of powdered racemic benzil, $\Delta\Delta H_{\text{fusion}} \neq 0$.

3) The angle between Earth's inertial spin and gravitational orbit rotates 360°/24 hours. This sources a composition Eötvös experiment signal. Add $P3_121$ and $P3_221$ benzil test masses aligned N-S and the coordinate frame cycles chiral, achiral, opposite chiral, achiral every 24 hours. A sinusoidal $\Delta\Delta \mathrm{H}_{\text{fusion}} \neq 0$ will appear.

4) (2)+(3). Physics contains no alternative explanation for this observation.

Compare EP parity violation experiments with classically opposed composition EP experiments, Be versus Ti or Mg, (nuclear binding energies)/baryon (Gundlach, 2005; Newman, 2001). Neutron and proton mass equivalents are weighted for isotopic abundance (Be is monoisotopic). A small (net difference)/(average active mass) fraction emerges,

p = 938.271998 MeV
n = 939.565330 MeV
Be = 6.462844 MeV/baryon binding energy
Mg = 8.265129 MeV/baryon binding energy

Ti = 8.714634 MeV/baryon binding energy
[Ti - Be]/[(30.9300n + 26p)/56.9300] = 0.002398 of total mass is active mass
[Mg - Be]/[(17.3202n + 16p)/33.3202] = 0.001919 of total mass is active mass

1.5 cm diameter, 4.68 g α-quartz single crystal test masses have $(1 - \chi) = 6\text{x}10^{-16}$ with (active mass)/(rest mass) > 0.9997. The parity experiment has a factor of 417 to 521 active mass fraction advantage over the largest active mass fraction composition experiments. 3 mm diameter, 17.7 mg benzil single crystal test masses have $(1 - \chi) = 2\text{x}10^{-14}$. Benzil has ΔH_{fusion} = 112 J/g at 95°C in a 0.1% precision differential scanning calorimeter. Given 10^{-13} difference/average Eötvös experiment divergence, parity calorimetry measures difference $|m_g - m_i|c^2$, 8.99 J/g or 8% divergence. Parity calorimetry is 41,000 times more sensitive than a composition Eötvös experiment for its larger fraction of active mass and for sensing mass-equivalent energy difference.

VI. CONCLUSION

Equivalence Principle violation tests are proposed using chemically and macroscopically identical, single crystal, maximum opposite parity atomic mass distributions: enantiomorphic crystallographic space groups $P3_121$ and $P3_221$ quartz (Eötvös, parity-sparing) or benzil (calorimetry, parity-destroying). Non-zero net outputs are consistent with teleparallel gravitation theory, spacetime torsion, and a massed sector chiral anisotropic vacuum background. Quantum gravitation theories require supplementing Einstein-Hilbert action with an odd-parity Chern-Simons term (Yunes and Finn, 2008) active only in the massed sector. Reproducible non-zero parity test outputs would falsify the EP, selectively falsifying metric gravitation theory (EP postulated), perturbative string theory (BRST invariance required), and conservation of angular momentum (isotropic vacuum plus Noether's theorem) for opposite parity atomic mass distributions. Biological homochirality was universally biased by residual chiral vacuum background. No prior achiral observation would be contradicted. Somebody should look.

REFERENCES

... (2001) *Planetary and Lunar Coordinates 2001-2020*, HM Nautical Almanac Office and Nautical Almanac Office of the United States Naval Observatory, ISBN: 0-943396-68-9.

Adenis, C., V. Langer, O. Lindqvist (1989) Reinvestigation of the structure of tellurium, *Acta Cryst. C* **45,** 941.

Aldrovandi, R. ,Tiago Gribl Lucas, J. G. Pereira, (2008a) Does a tensorial energy-momentum density for gravitation exist?, *arxiv:0812.0034*.

Aldrovandi, R., J. G. Pereira (2007) Gravitation: in search of the missing torsion, *Ann. Fond. Louis de Broglie* **32,** 229, *arxiv:0801.4148*.

Autschbach, J. (2009) Department of Chemistry, State University of New York/Buffalo, private communication.

Auvray, P., F. Genet (1973) Affinement de la structure cristalline du cinabre a-HgS, *Bull Soc. Franc. Mineral. Cristall*. **96,** 218.

Barron, L. D. (1981) Optical activity and time reversal, *J. Mol. Phys*. **43**, 1395.

Champion, D. J., et al. (2008) An Eccentric Binary Millisecond Pulsar in the Galactic Plane, *arxiv.org:0805.2396*.

Contaldi, C. R., J. Magueijo, L. Smolin, (2008) Anomalous CMB Polarization and Gravitational Chirality, *Phys.Rev.Lett.*101, 141101, arxiv:0806.3082v1.

Crawford, T. D., M. C. Tam, M. L. Abrams (2007) The Current State of Ab Initio Calculations of Optical Rotation and Electronic Circular Dichroism Spectra, *J. Phys. Chem. A* **111**(48), 12057.

Einstein, A. (1907) *Jahrbuch der Radioaktivität u. Electronik* **4,** 411; *The Collected Papers of Albert Einstein*, Vol. 2 English translation, A. Beck, trans. (Princeton University Press: Princeton, NJ, 1989) p. 252.

Etxebarria, J., C. L. Folcia, and J. Ortega (2000) Origin of the optical activity of silver thiogallate, *Appl. Cryst*. **33**, 126.

Flack, H. D. (2003) Chiral and achiral crystal structures, *Helv. Chim. Acta* **86**, 905.

Glazer, A. M., K. Stadnicka (1986) On the origin of optical activity in crystal structures, *J. Appl. Cryst.* **19**, 108.

Gundlach, J.H. (2005) Laboratory tests of gravity, *New J. Phys.* **7** 205.

Hargittai, I., Hargittai, M. (1995) *Symmetry through the eyes of a chemist,* 2nd Edition (Springer), pp. 75-78.

Heckel, B. R., C. E. Cramer, T. S. Cook, E. G. Adelberger, S. Schlamminger, and U. Schmidt (2006) New CP-Violation and Preferred-Frame Tests with Polarized Electrons, *Phys. Rev. Lett.* **97**, 021603;

Hooper , J.W., (….) BigCHI programme, MazePath Software, Farmington Hills, MI; Anne Marie Merritt, VMware Inc., Palo Alto, CA; and Anthony J. Lapen , Harvard Apparatus, Holliston, MA. CHIpir programmed by John Edward Scott, Daedalus Solutions, London.

Hou, L-S., W-T. Ni, Y-C. M. Li (2003) Test of cosmic spatial isotropy for polarized electrons using a rotatable torsion balance, *Phys. Rev. Lett.* **90**, 201101;

Jerphagnon, J., D. S. Chemla, (1976) Optical activity of crystals, *J. Chem. Phys*. **65**(4), 1522;

Keszthelyi, L. (2003) Parity-violating energy difference between enantiomers: recent developments, *Mendeleev Commun*. **13**(3), 129.

Kihara, K. (1990) An X-ray study of the temperature dependence of the quartz structure, *Eur. J. Mineralogy* **2**, 63.

Lee, T. D., Yang, C. N. (1956) Question of Parity Conservation in Weak Interactions, *Phys. Rev.* **104**, 254.

Mercuri, S. (2006) Fermions in the Ashtekar-Barbero connection formalism for arbitrary values of the Immirzi parameter, *Phys. Rev. D* **73**, 084016.

Mezey, P. G. (1995) Rules on chiral and achiral molecular transformations, *J. Math. Chem*. **17**, 185.

More, M., G. Odou, J. Lefebvre (1987) Structure Determination of Benzil in its Two Phases, *Acta Cryst. B* **43**, 398.

Murphy, Jr., T.W., E.G. Adelberger, J.B.R. Battat, et al. (2007) APOLLO: the Apache Point Observatory Lunar Laser-ranging Operation: Instrument Description and First Detections, *arxiv:0710.0890v2*.

Nakazaki, M., H. Chikamatsu, M. Taniguchi (1982) Horse Liver Alcohol Dehydrogenase (HLADH) Mediated Chemicoenzymatic Asymmetric Synthesis of (+)-Twistane from cis-Decalin-2,7-dione, *Chem. Lett.* **11**[11], 1761.

Newman, R. (2001) Prospects for terrestrial equivalence principle tests with a cryogenic torsion pendulum, *Class. Quantum Grav*. **18**, 2407.

Pagni, R.M., R. N. Compton (2002) Asymmetric Synthesis of Optically Active Sodium Chlorate and Bromate Crystals, *Crystal Growth & Design* **2**(4), 249.

Petitjean, M. (1999) On the root mean square quantitative chirality and quantitative symmetry measures, *J. Math. Phys.* **40**, 4587, petitjeanmichel.free.fr/itoweb.petitjean.freeware.html#QCM

Petitjean, M. (2002) Chiral mixtures, *J. Math. Phys*. **43**, 4147.

Petitjean, M. (2003) Chirality and symmetry measures: A transdisciplinary review, *Entropy* **5**, 271.

Quack, M. (2002) How Important is Parity Violation for Molecular and Biomolecular Chirality?, *Angew. Chem. Int. Ed*. **41**(24), 4618.

Ritter, R. C., C. E. Goldblum, W-T Ni, G. T. Gillies, C. C. Speake (1990) Experimental test of equivalence principle with polarized masses, *Phys. Rev. D* **42,** 977.

Schlamminger, S., K.-Y. Choi, T. A. Wagner, J. H. Gundlach, and E. G. Adelberger, (2008) Test of the Equivalence Principle Using a Rotating Torsion Balance, *Phys. Rev. Lett*. **100**, 041101.

Schwartz, A. M. (2004) Affine vs. Metric Gravitation Parity Test, Abstract D9.006, *Bull. Am. Phys. Soc.*, **49**[2], 54.

Schwartz, A. M., Petitjean, M. (2008) [6.6]Chiralane: A remarkably symmetric chiral molecule, *Symmetry: Culture and Science* 19, 4, 307-316.

Smith, P. (…) Personal communication, Mathematics Dept., Lehigh University.

Szivessey, G. and C. Münster (1934) Über die Prüfung der Gitteroptik bei aktiven Kristallen, **Ann. Phys.** (Leipzig) **20**, 703.

Tsuda, M. and T. Shirafuji, (1996) Consistency of matter field equations in Ashtekar formulation, *arxiv:gr-qc/9602022*.

Wiberg, K., Y-G Wang, S. Wilson, P. Vaccaro, J. Cheeseman (2006) Sum-over-States Calculation of the Specific Rotations of Some Substituted Oxiranes, Chloropropionitrile, Ethane, and Norbornenone, *J. Phys. Chem. A* **110**(51), 13995.

Wigner, E. (1960) The Unreasonable Effectiveness of Mathematics in the Natural Sciences, *Comm. Pure Appl. Math* **13**(1), 1.

Will, C. M. (2005) The Confrontation between General Relativity and Experiment, *Living. Rev. Rel.* **9**, 3; arxiv:gr-qc/0510072v2;

Wright, A. F. and M. S. Lehmann (1981) The structure of quartz at 25 and 590 degrees C determined by neutron diffraction, *J. Solid State Chem*. **36**, 371.

Yogev-Einot, D. and D. Avnir (2003) Quantitative Symmetry and Chirality of the Molecular Building Blocks of Quartz, *Chem. Mater*. **15**, 464.

Yunes, N., L. S. Finn (2008) Constraining effective quantum gravity with LISA, *arXiv:0811.0181v1*.